Journal of The Electrochemical Society, **163** (6) F485-F491 (2016)
0013-4651/2016/163(6)/F485/7/$33.00 © The Electrochemical Society

Acid-Doped ABPBI Membranes Prepared by Low-Temperature Casting: Proton Conductivity and Water Uptake Properties Compared with Other Polybenzimidazole-Based Membranes

Liliana A. Diaz,[a,b] Graciela C. Abuin,[b] and Horacio R. Corti[a,z]

[a]*Departamento de Física de Materia Condensada, Centro Atómico Constituyentes, Comisión Nacional de Energía Atómica (CNEA), B1650KNA San Martín, Buenos Aires, Argentina*
[b]*Instituto Nacional de Tecnologia Industrial (INTI), B1650KNA San Martín, Buenos Aires, Argentina*

Phosphoric acid doped ABPBI (poly [2,5-benzimidazole]) membranes were prepared with a new low temperature casting procedure (ABPBI-ET), and their water uptake and proton conductivity were measured. The results were compared with those of ABPBI casted at high temperature (ABPBI-MSA), poly [2-2′-(m-phenylene)-5-5′ bibenzimidazole] (PBI), and commercial cross-linked Fumatech ABPBI (ABPBI-C) membranes. The water uptake of ultra thin ABPBI-ET membranes in the range 7–30 nm supported over gold substrate, was also measured and compared with PBI ones. The in-plane proton conductivities of all the membranes were measured in the temperature range from 20° to 120°C at different water activities. The ABPBI-ET doped in 10.6 M H_3PO_4 and ABPBI-C doped in 14.9 M H_3PO_4 showed the highest conductivities, even higher than those reported for Nafion membranes. ABPBI-ET membranes showed a maximum as a function of water activity at $a_w \approx 0.55$, a behavior that can be rationalized in terms of the dissociation constant of the ABPBI-H_3PO_4 complexes calculated using the Scatchard method, and the H_3PO_4 concentration in the water inside the membrane.

Manuscript submitted January 12, 2016; revised manuscript received February 12, 2016. Published March 9, 2016.

Nafion, a perfluorinated sulfonic acid ionomer, is commonly used in Proton Exchange Membrane (PEM) fuel cells operated at room and moderate temperatures (lower than 100°C) due to its excellent proton conductivity and chemical stability.[1] The main disadvantages related to this type of fuel cells are certainly the need of feeding a high purity hydrogen stream at the anode and the low efficiency of the oxygen reduction reaction (ORR) at the cathode. Both problems can be ameliorated by increasing the operation temperature of the PEM fuel cells above 100°C.[2,3] Nafion is not an appropriated proton exchange membrane for this purpose because it dehydrates, and its proton conductivity goes down at temperatures above 100°C.[4–6]

An alternative PEM for high temperature fuel cells is poly[2,2′-(phenylene)-5,5′-bibenzimidazole] (PBI), a non-ionic polymer, stable at high temperature that becomes a proton conductor when doped with a strong acid, such as sulfuric or phosphoric acid. Commercial PBI is a proprietary product from Celanese prepared from 3,3′,4,4′-tetra aminobiphenyl (TAB) and diphenyl isophtalate.[7] A modified PBI polymer, poly[2,5-benzimidazole] (ABPBI), has been synthesized by condensation of 3,4-diaminobenzoic acid (DABA) monomer in polyphosphoric acid,[8] and by polymerization of DAB or tetra-aminobencene with pyridine-dicarboxylic or naphtalene-dicarboxylic acids.[7,9] The chemical structure of these polymers is depicted in Figure 1.

A new sol-gel process for synthesizing high molecular weight PBI in polyphosphoric acid (PPA) at 200°C was developed by Xiao et al.,[10] and a modified version of this process was used by BASF Fuel Cells to produce commercial phosphoric acid doped PBI membranes (Celtec V).[11]

Proton conductivity of acid-doped PBI has been studied under different conditions of membrane preparation, H_3PO_4 doping level, defined as the moles of acid per mole of imidazole ring (λ_a), temperature, and water activity.[2,9,10,12–28] A comparison of the results is not simple due to temperature or acid doping level differences. However, it can be observed that dry PBI membranes ($a_w = 0$) exhibit very low specific conductivities ($\sigma < 1$ mS.cm^{-1}) for doping levels $\lambda_a \leq 1.5$, and moderate conductivities ($\sigma \leq 23$ mS.cm^{-1}) for $\lambda_a \geq 3.0$ and temperatures close to 200°C. Under ambient conditions a small increment in membrane humidity takes place,[15] resulting in an important increase in conductivity, particularly at high doping levels.[18] PBI membranes with $\lambda_a > 3.0$ and at high humidity conditions have proton conductivities similar to that found for Nafion membranes (around 100 mS.cm^{-1}) above 150°C.

In addition, it is observed that the solvent used to prepare the membrane by casting has a great influence on its conductivity, probably due to the formation of different polymer microstructures. Porosity in the microstructure of PBI has been created by leaching out porogens, like phthalates or phosphates, from PBI/porogen films,[25] or using a hard template (silica nanoparticles 13 nm in diameter).[26] However, the best results so far were obtained for PBI membranes prepared using the PPA sol- gel process.[10] This procedure leads to very high acid doping levels and the conductivity of a membrane with $\lambda_a \approx 16$, raises from 10 mS.cm^{-1} at room temperature up to 260 mS.cm^{-1} at 200°C. The last value is comparable with those observed for the best proton conducting Nafion/inorganic composite membranes at temperatures above 100°C.

Crosslinked PBI membranes have been proposed for improved mechanical strength and chemical stability.[27,28] These membranes exhibit conductivities close to 98 mS.cm^{-1} at 180°C and high acid doping at $a_w = 0.1$,[27] and 64 mS.cm^{-1} at 170°C under dry conditions ($a_w = 0$).[28]

The conductivity data reported in the literature for ABPBI membranes include those obtained by casting,[9,13,19,29–35] along with results for commercial crosslinked ABPBI membranes,[13,36] an isomer of ABPBI,[37] sulfonated ABPBI,[19,29] and ABPBI composites.[19,33,38] Most of the membranes were prepared by casting from methanesulfonic acid (MSA) and dry ($a_w \approx 0$) ABPBI membranes reach a maximum conductivity close to 25 mS.cm^{-1}, for doping degree $\lambda_a = 2.7$ at 185°C.[19,29,31,33]

An isomer of ABPBI which contains head-to head and tail-to-tail benzimidazole sequences, was recently synthetized,[37] and membranes were prepared by using the PPA sol-gel process. The membranes, like those prepared with PBI using this method,[10] have a much higher doping degree and their conductivities are above 200 mS.cm^{-1} at 180°C, even without humidification. Proton conductivities above 200 mS.cm^{-1} were also reported for commercial crosslinked ABPBI membranes by Fumatech,[36] at 120 and 140°C

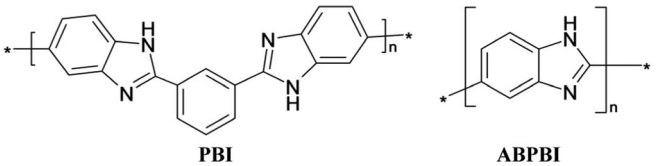

Figure 1. Chemical structure of PBI and ABPBI polymers.

[z]E-mail: hrcorti@cnea.gov.ar

and partial humidification. ABPBI composites with other polymers exhibit only modest conductivities.[19,33,38]

The picture emerging from the reported data is that ABPBI membranes seem to have similar or higher proton conductivity than PBI membranes. However, a reliable comparison between conductivities of PBI and ABPBI is prevented by differences parameters that determine the proton transport in these polymers, namely, level of acid doping, humidity (or water uptake), temperature, and membrane microstructure, which in turns depend on the method of membrane preparation.

The main goal of this work is to study the proton conductivity of ABPBI membranes prepared by a new casting procedure at low temperature using alkalinized ethanol as a solvent, and to compare the results with those obtained for ABPBI membranes casted at high temperature, commercial ABPBI membranes, and also with membranes obtained from commercial PBI. The proton conductivity will be analyzed on the basis of the acid dissociation of the PBI or ABPBI complexes with phosphoric acid, using the procedure developed by Scatchard et al.,[39] already used by He et al.,[40] for describing the conductivity of acid doped PBI membranes.

Experimental

ABPBI synthesis and membrane preparation.—ABPBI polymer, whose chemical structure is shown in Figure 1 along with that of PBI, was synthesized by condensation of 3,4-diaminobenzoic acid (DABA) monomer in polyphosphoric acid (PPA) according to the procedure described by Ascencio et al.[11] The details of the procedure and post-synthesis polymer treatment have been reported elsewhere.[13,41]

Two casting procedures were employed to prepare membranes from the neutral polymer. In the high temperature casting a 5 wt% ABPBI solution in methanesulfonic acid was heated at 170 °C on a glass plate for few hours to evaporate the solvent, and the membrane was separated from the glass support by immersion in water. We call these membranes ABPBI-MSA.

The low temperature casting was performed from a solution of 4.2 wt% ABPBI and 2.7 wt% NaOH in ethanol on a Teflon plate, cooled with vapor from a liquid N_2 vessel in order to obtain a low evaporation rate. The temperature of the substrate was close to 0°C and the evaporation of the solvent overnight leads to the formation of a homogeneous membrane. We call these membranes ABPBI-ET.

PBI membranes were prepared by casting from a 5 wt% solution of PBI powder (Goodfellow) in dimethylacetamide (DMAc) in a vacuum furnace at 80 °C during 4 hours.

All the casted PBI and ABPBI membranes, having thickness between 50 and 150 μm, were doped in 10.6 M H_3PO_4 for 72 hours in order to protonate the imidazole ring. The same doping procedure was used with the commercial crosslinked ABPBI membranes Fumapem A (Fumatech). We call these membranes ABPBI-C.

Thicknesses of membrane samples used in the proton conductivity experiments were measured by means of a Mahr XL1-57B-15 dead load gauge.

Supported ultrathin ABPBI-ET membranes were also prepared by casting from ethanol/NaOH solutions on the gold electrode of a quartz crystal microbalance (QCM). The thicknesses of these membranes were determined by using AFM (Veeco–DI Multimode Nanoscope IIIa), as described previously.[42]

N,N-dimethylacetamide (Merck), H_3PO_4 (Merck), H_2O_2 (Merck), H_2SO_4 (Baker Analized), 3,4-diaminobenzoic acid, 97% (Aldrich), polyphosphoric acid 85% (Aldrich), methanesulfonic acid 99.5+% (Aldrich) and methanol (J.T.Baker) all analytical grade were used as received. Water was deionized and passed through a Millipore filter.

Proton conductivity.—Previously to the ionic conductivity measurements, each membrane was equilibrated in isopiestic equilibrium inside sealed flasks with different salt saturated solutions at fixed water activity, at 25°C.

The "in plane" ionic conductivities of the membranes were measured by resorting to a 4-electrode cell depicted in Figure 2. The membranes were cut in strips (1 cm width and 3 cm length). The polarization electrodes (A and B) were platinum strips around 2 mm width, while the measurement electrodes were platinum wires (C and D) 0.5 mm in diameter, all of them attached to a PTFE plate around 1 cm width and 5 mm thick. The membrane was located between the PTFE plate including the electrodes and a second PTFE plate having thicker thickness. Both PTFE plates had three holes (6 mm in diameters) to allow the membrane to be exposed to water vapor when enclosed in a glass vessel thermostatized at the working temperature, sandwiched between two steel plates with the corresponding holes (matching those on the PTFE plates) to assure the assembly rigidity. The electrodes were in good contact with the membrane owing to the pressure applied by two bolts located in the cell extremes, as indicated in Figure 2. The temperature was controlled by a digital controller N621283 Fadri using a PTR100, located into the cell, as temperature sensor. The samples electrical resistances were measured using an AutoLab PGSTAT 302 N potentiostat-galvanostat in galvanostatic mode. A current of 10 μA (frequency range 50 Hz–100 kHz) was applied between the polarization electrodes, while the potential drop between the internal electrodes was measured. The specific conductivity of the membrane was calculated from the measured resistance, R, using the equation:

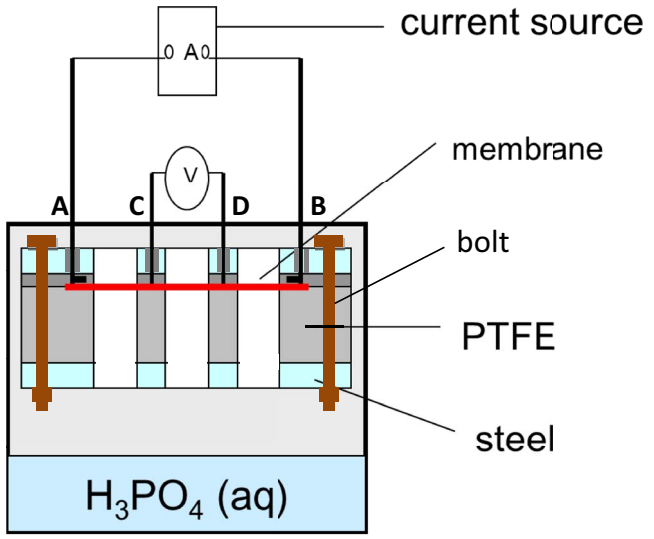

Figure 2. Scheme of the 4-electrodes conductivity cell, showing the polarization (A and B) and measurement (C and D) electrodes.

$$\sigma = \frac{l}{R\delta b} \qquad [1]$$

where l is the distance between the measurement (C-D) electrodes, δ is the membrane thickness, and b is the membrane width.

Molecular weight, phosphoric acid doping level and water uptake.—The molecular weights of the synthesized polymers were determined from viscosity measurements of their solutions in concentrated 96 wt% H_2SO_4 using a Cannon – Fenske 150 viscosimeter, as described previously.[41]

Phosphoric acid uptake of ABPBI-ET ethanol casted and ABPBI-C membranes was measured employing the method previously described.[41] The membrane samples doped in 10.6 M aqueous H_3PO_4 were isopiestically equilibrated at 25°C with the acid solution in capped and sealed polypropylene flasks. Once the samples reached constant weight, they were immersed in 0.1 M KCl aqueous solutions until a constant pH value was reached. The total H_3PO_4 uptake was calculated from the volume of NaOH solution added between the two step pH jumps, corresponding to the first and second dissociation of the acid, during the titration. The doping degree, λ_a, is defined as the number of moles of acid, n_a, in the membrane per mol of monomer

unit containing one imidazole ring:

$$\lambda_a = \frac{n_a M_p}{m_p} \quad [2]$$

where m_p is the mass of polymer, and M_p is the monomer mass (M_p = 142 g · mol^{-1} in the case of PBI and M_p = 116 g · mol^{-1} for ABPBI).

The free acid content of the membrane, λ_f, represents the moles of free acid per imidazole ring, and it was calculated from the pH difference of the KCl solution before and after the membrane immersion.

In a previous work we have reported the water uptake of PBI and ABPBI membranes prepared by a high-temperature casting, similar to that reported here as ABPBI-MSA, and a low-temperature casting using formic acid as solvent.[41] The membranes prepared with the later procedure absorbed too much water and exhibited poor mechanical properties. For this reason we developed in this work a new low-temperature casting based in the use of ethanol/NaOH.

The water uptake of the ABPBI-ET ethanol casted and ABPBI-C membranes was measured as a function of the water activity, a_w, defined as the ratio between the water vapor pressure in the membrane to the vapor pressure of pure water at a given temperature. The water uptake at 30°C, for $0.15 < a_w < 1$, was determined from the difference of weight of the membranes in isopiestic equilibrium with saturated salt solutions and the weight, m_p, of the dry membrane without acid.

The water uptake is finally expressed as λ_w, the ratio between the total moles of water, n_{H2O}, sorbed per mol of monomer unit containing one imidazole ring.

$$\lambda_w = \frac{n_{H2O} M_p}{m_p} \quad [3]$$

Alternatively, the water uptake can be expressed as the mass of water sorbed, m_s, per gram of dry polymer, $m = m_s / m_p$.

Other parameter employed for measuring the water uptake, referred to the amount of acid in the membrane, is the number of water molecules per molecule of phosphoric acid, λ_{wa}, calculated through the expression:

$$\lambda_{wa} = \frac{m_s M_a}{m_a M_w} \quad [4]$$

where m_a is the mass of acid in the membrane, and M_w = 18.016 g.mol^{-1}, M_a = 98.00 g.mol^{-1}, are the water and acid molecular weight, respectively.

The water uptake of ultrathin membranes was performed by the QCM method described elsewhere.[13] The QCM was located in a chamber in order to control the relative humidity of the membrane. The mass of the dry membrane was determined by flowing dry nitrogen through the chamber, until a constant mass was measured. Then the nitrogen stream was bubbled through saturated salt solutions of known water activity and the change in mass was determined. Due to the nanoscale of the films the sorption equilibrium in these experiments was reached after a few minutes.

Results and Discussion

Molecular weight of PBI and ABPBI.—From the intrinsic viscosities measured in concentrated H_2SO_4, and, using the Mark-Houwink-Sakurada equation,[41] we obtained the molecular weights 18,800 gmol^{-1} for ABPBI and 19,600 gmol^{-1} for PBI.

Phosphoric acid doping level.—The phosphoric acid uptake and the free acid content of the ABPBI-MSA, ABPBI-ET, ABPBI-C, and PBI polymers, measured in terms of acid moles per repetitive unit, are summarized in Table I.

The acid doping levels of the ABPBI membranes from aqueous 10.6 M H_3PO_4 are higher than that found for PBI, except for the case of ABPBI-C, where the doping level is similar to that reported by Wannek et al. from a 10 M H_3PO_4 aqueous solution (λ_a = 1.80).[36] This is probably due to the crosslinked nature of the commercial ABPBI membrane that makes the complex formation more difficult by shifting the osmotic equilibrium. We observed that ABPBI-C reaches doping levels similar to that found in our ABPBI membranes when doped in 14.9 M H_3PO_4 aqueous solution. It should be mentioned that our ABPBI membranes cannot be doped in 14.9 M H_3PO_4, because they are not stable and start to dissolve when immersed in such a concentrated media.

Table I. Doping degree (λ_a), free acid content (λ_f) and water content per molecule of acid (λ_{wa}), at 25 °C for PBI and ABPBI membranes doped in 10.6 M aqueous H_3PO_4.

Membrane	λ_a	λ_f	λ_{wa}
ABPBI–ET	2.5	0.095	1.82
ABPBI–MSA	2.8[a]	0.093[a]	0.78[a]
ABPBI–C	1.55	0.022	2.19
	3.1[b]		
PBI	1.9[a]	0.095[a]	1.14[a]

[a]From Ref. 41.
[b]Doped in H_3PO_4 14.9 M.

The free acid contents of all the membranes are less that 0.1 and are similar for PBI and the ABPBI membranes prepared in this work.

It is worth to analyze the behavior of the number of water molecules per molecule of phosphoric acid, λ_{wa}, also shown in Table I, which will be used later in the discussion of proton conductivity. This parameter is much higher for ABPBI-ET and ABPBI-C, indicating a relative more dilute phosphoric acid within the membrane, as compare to ABPBI-MSA and PBI.

Water uptake.—The water sorption isotherm of the ABPBI-ET membranes at 30°C, expressed as m, the mass of water per mass of dry membrane, is shown in Figure 3 along with previously reported data for PBI and ABPBI-MSA, for comparison. The water uptake of ABPBI-ET is higher than that of PBI all over the water activity range, while it is also higher than that of ABPBI-MSA at a_w <0.7. The water uptake of ABPBI-C membranes doped in 14.9 M H_3PO_4, also included in Figure 3, is higher than those of the rest of membranes studied.

As previously observed for PBI, and ABPBI-MSA, the water isotherm for ABPBI-ET can be represented with the Guggenheim-Anderson-de Boer (GAB) equation,[43]

$$\frac{a_w}{m(1 - f a_w)} = \frac{1}{f m_0 c} + \frac{(c+1)}{m_0 c} a_w \quad [5]$$

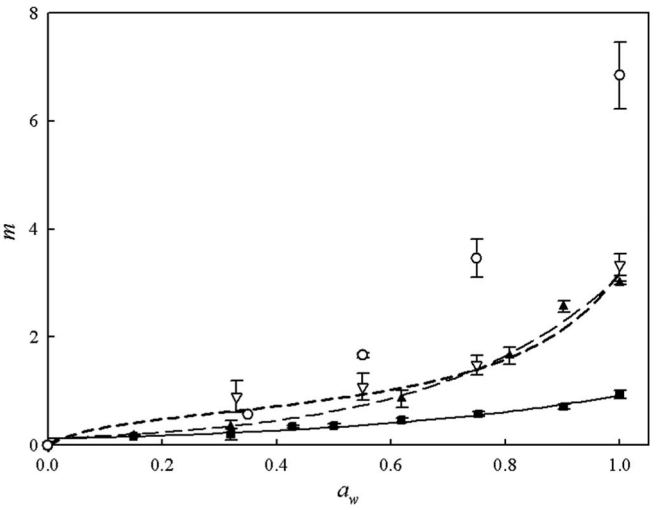

Figure 3. Water sorption isotherm, expressed as m vs. a_w, at 30°C: (■) PBI (λ_a = 1.9); (▲) ABPBI − MSA (λ_a = 2.8); (▽) ABPBI − ET (λ_a = 2.5), (○) ABPBI – C (λ_a = 3.1). The lines correspond to the fit of the isotherms using GAB Eq. 5, using the parameters of Table II.

Table II. Parameters of the GAB isotherms for PBI, ABPBI-MSA, and ABPBI-ET membranes.

GAB parameters	PBI	ABPBI-MSA	ABPBI-ET
m_o	0.30 ± 0.02	1.37 ± 2.10	0.55 ± 0.72
c	8.83 ± 2.34	0.95 ± 1.73	13.1 ± 2.4
f	0.69 ± 0.02	0.69 ± 0.20	0.83 ± 0.02
Standard deviation	0.006	0.067	0.046

where m is the water uptake expressed as the mass of water sorbed per gram of dry polymer, and the three adjustable parameters are: m_0, the mass of water at the monolayer per gram of dry membrane, $c = \exp[(E_1\text{-}E_L)/RT]$, and $f = \exp[(E_2 - E_L)/RT]$. The last two parameters are related to the differences between the pure water liquefaction energy (E_L) and the interaction energy of water in the monolayer (E_1) and the layers on top of the monolayer (E_2) with the polymer-H_3PO_4 complex, respectively. The meaning of these parameters have been discussed elsewhere.[41] We only note here that: i) m_0 corresponds to the mass of the water monolayer sorbed on the polymer, like in the Langmuir isotherm, and ii) the GAB Eqn. 5 becomes the BET equation when $f = 1$, that is, for all the water layers top of the monolayers having the same interactions.

As observed in Figure 3 for ABPBI-ET, the GAB equation provides a reasonable fit of the isotherm data (standard deviation = 0.046), yielding the parameters summarized in Table II. The water monolayer complete at $a_w = 0.25$ in ABPBI-ET, similarly to that observed for PBI ($m_0 = 0.30$). For ABPBI-ET the parameter c is much higher than for ABPBI –HT, which indicates a strong interaction of water with the ionic parts of the polymer for the low temperature casted membrane, as also found in PBI ($c = 8.8$).[41] The parameter f for ABPBI-ET is slightly lower than unity, that is, the isotherm can be approximated by the BET model at low water activities, but it exhibits a finite water sorption at saturation ($a_w = 1$).

In PEM fuel cell applications the carbon-supported catalyst layer is applied on the membrane using an ink prepared with the same membrane ionomer as a binder. Thus, the thickness of the ionomer films covering the catalysts is usually thinner than 1 μm, and the knowledge of the water sorption properties of ultrathin films is useful for modeling the three-phase region of a PEM fuel cell.

In Figures 4a and 4b are shown the water sorption isotherms of the ultrathin ABPBI-ET and PBI membranes with thickness between 7–30 nm and 7–25 nm, respectively. For both type of polymers the water uptake by the ultrathin membranes is much lower than that of the massive membrane all over the water activity range. It is interesting to note that the sorption of the thinnest membranes (7–9 nm thick) is higher than membranes having thickness in the range 10–30 nm. This could be explained by the existence of a water rich layer between the membrane and the gold substrate,[44,45] or due to an inhomogeneous covering of the substrate. In the last case the uncovered gold substrate would adsorb a considerable amount of water, leading to an overestimation of the water uptake by the supported membrane. For membranes with thickness above 10 nm, where the coverage of the substrate is expected to be complete, the water uptake is 3 to 5 times lower than that of the bulky membranes. Certainly this is a nano-confinement effect that will be analyzed in more detail in a forthcoming study.

Proton conductivity.—Figure 5 shows the specific conductivity of ABPBI-ET membranes as a function of temperature at four water activities between 0.33 and 1.00. As expected, the conductivity increases with increasing temperature, but it is worthy to note that the higher conductivities are observed at $a_w = 0.55$, instead of at $a_w = 1.0$ as we will show for the rest of the membranes. This fact is more evident when the conductivity is plotted as a function of water activity, as shown in Figure 6. Clearly, the conductivity at the maximum increases with temperature, meanwhile at $a_w = 1.0$, the conductivity is essentially similar at temperatures above 30°C, probably as a consequence of membrane dehydration.

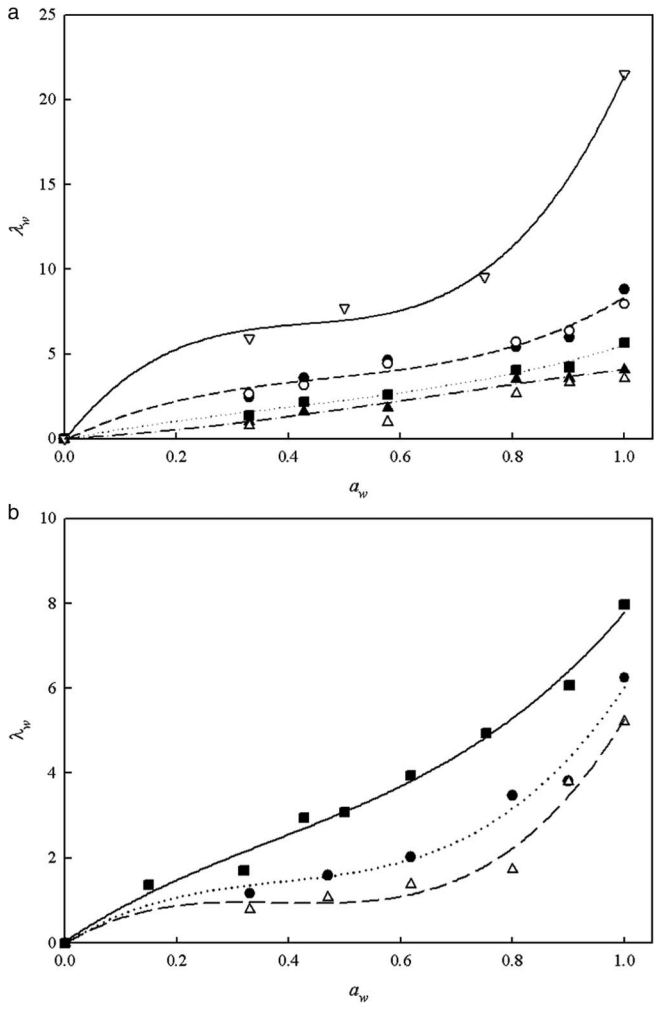

Figure 4. Water sorption isotherm, expressed as λ_w vs. a_w, at room temperature for (a) ABPBI-ET membranes: (▽) massive; (●) 7 nm; (○) 9 nm; (△) 18 nm; (▲) 19 nm; (■) 30 nm. (b) PBI membranes: (■) massive; (●) 7 nm; (△) 25 nm.

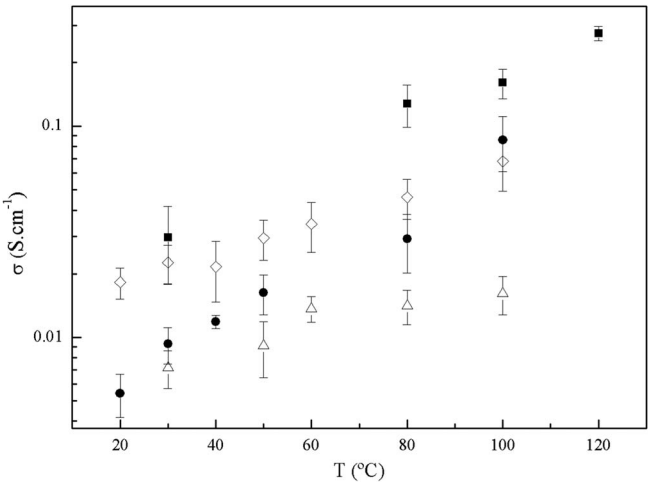

Figure 5. Proton conductivity of ABPBI-ET membranes as a function of temperature at different water activities: (●) $a_w = 0.33$; (■) $a_w = 0.55$; (◇) $a_w = 0.75$; (△) $a_w = 1$.

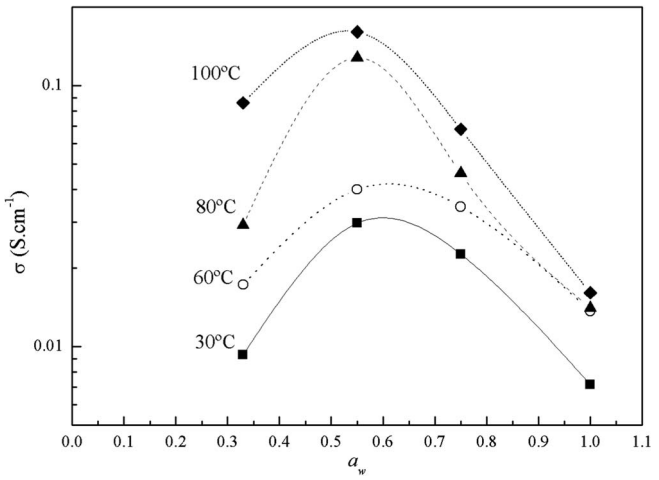

Figure 6. Proton conductivity of ABPBI-ET membranes as a function of water activities at several temperatures.

The proton conductivity of ABPBI-ET is compared to the other membranes in Figure 7, at $a_w = 0.33$. The conductivities of ABPBI-MSA, PBI and ABPBI-C membranes doped in 10.6 M H_3PO_4, are lower all over the range of temperatures studied, and the differences in relation with ABPBI-ET are more evident when temperature is close or above 100°C. The commercial membrane (ABPBI-C) doped in more concentrated (14.9 M) phosphoric acid ($\lambda_a = 3.1$) also plotted in Figure 7, exhibits enhanced conductivity, similar to that for ABPBI-ET at $a_w = 0.55$. The conductivity of ABPBI-C agrees with that reported by Wannek et al. at the same acid doping level.[36]

In summary, at temperatures above 80°C and similar doping degree, ABPBI-ET and ABPBI-C membranes exhibit proton conductivities over 0.1 $S.cm^{-1}$ at different water activities. This conductivity values are higher than those observed for Nafion membranes over the temperature range analyzed in this work, and the proton conductivity is expected to be even higher above 120°C.

Dissociation constants of ABPBI-H_3PO_4 complexes.—In order to rationalize differences between the proton conductivity behavior of ABPBI membranes as compared to PBI ones, we will perform a thermodynamic analysis similar to that described by He et al.[40] using the Scatchard method.[39] Briefly, He et al. considered that H_3PO_4 forms a complex with the –N = group of the imidazole ring (L_1 site) which lead to the protonation of the ring. This complex can dissociate according to the equilibrium:

$$L_1 - H_3PO_4 = L_1 + H_2PO_4^- + H^+$$

The corresponding equilibrium constant K_{aL1} can be expressed as the ratio between the first dissociation constant of H_3PO_4 (K_{a1}), and the equilibrium constant, K_{L1}, of the complex formation ($L_1 + H_3PO_4 = L_1$–H_3PO_4).

Once the L_1 site is saturated with H_3PO_4, a new hydrogen bonding may form with the –NH– group of the imidazole ring and the acid or between H_3PO_4 molecules. Both types of bonding sites are referred as L_2 site. A similar equilibrium to that written for site 1 leads to the equilibrium constant K_{aL2}, which again can be expressed as the ratio between the first dissociation constant of H_3PO_4 (K_{a1}) and the equilibrium constant, K_{L2}, of the complex formation ($L_2 + H_3PO_4 = L_2$–H_3PO_4).

By using the acid doping level at different H_3PO_4 concentrations, He et al. obtained $K_{L1} = 12.7$ and $K_{L2} = 0.19$ for PBI membranes using the Scatchard method.[40] Thus, they calculated the values $K_{aL1} = 5.4\ 10^{-4}$, and $K_{aL2} = 0.036$ for the dissociation constant of the complexes.

We adopted the same method to obtain the dissociation constant for ABPBI-MSA acid complexes, by resorting to the doping level vs. acid concentration in doping solution data reported by Asencio et al.[30,33] The Scatchard method fit reasonably well the experimental data up to 12.6 M H_3PO_4 in doping solution. The results, shown in Table III, indicate that H_3PO_4 has a lower affinity for the L_2 sites in ABPBI as compared to PBI, while the affinity for L_1 sites are not too different, although is lower in ABPBI-MSA. The dissociation constant of the ABPBI- H_3PO_4 complexes, included in Table III, indicate that the dissociation of the L_1 site in ABPBI is almost twice that of PBI, while the dissociation of the L_2 site in ABPBI is 13 times higher than that measured for PBI.

Therefore, it can be concluded that the Grotthuss mechanism of proton conduction is favored in sites L_2 of ABPBI as a results of a higher dissociation as compared to the same sites in PBI. The differences for sites L_1 are less important, but reinforce the trends. In summary, the observed differences in the dissociation of the complexes could explain the higher conductivity observed in Figure 7 for ABPBI-MSA membranes at room temperature, as compared to PBI.

We have found that the data reported by Asencio et al.[30–33] can be fitted with the multilayer sorption model based in the BET equation all over the range of acid concentrations of the doping solution. The calculated doping grade for the first multilayer is 0.94 acid molecules per repeating polymer unit.

He et al.[40] defined a limiting doping level, $[L^1]_T$, as the maximum doping level related with H_3PO_4 molecules linked to L_1 sites. According to them, the acid molecules that take part in the proton conduction in PBI membranes are that linked to L_2 sites.[46] Acid molecules linked to L_1 sites can be neglected as they are occluded and play no role in the proton conduction mechanism. In order to test if this assumption can be applied to the ABPBI membranes, we have estimated that $[L^1]_T = 1.02 \pm 0.08$.

Figure 8 shows the proton conductivity vs. the acid concentration inside the membrane (calculated from acid uptake, λ_a, and water uptake, λ_w), along with the conductivity of phosphoric acid aqueous solution at 25°C as a function of the acid concentration.[47] The acid

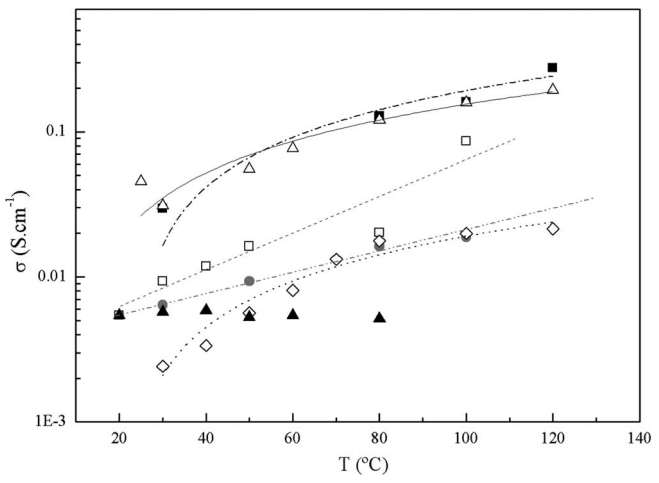

Figure 7. Comparison of the proton conductivities of ABPBI and PBI membranes at $a_w = 0.33$: (□) ABPBI-ET ($\lambda_a = 2.5$); (●) ABPBI-MSA ($\lambda_a = 2.8$); (▲) ABPBI-C ($\lambda_a = 1.55$); (△) ABPBI-C ($\lambda_a = 3.1$); (◇) PBI ($\lambda_a = 1.9$). Also plotted the conductivity of (■) ABPBI-ET ($\lambda_a = 2.5$) at $a_w = 0.55$.

Table III. Equilibrium constant of formation and dissociation of the phosphoric acid PBI-and ABPBI complexes.

	Complex formation		Complex dissociation	
Equilibrium constant	K_{L1}	K_{L2}	K_{aL1}	K_{aL2}
PBI-H_3PO_4	12.7	0.19	$5.4 \cdot 10^{-4}$	0.036
ABPBI-MSA-H_3PO_4	6.64	0.013	$9.5 \cdot 10^{-4}$	0.48

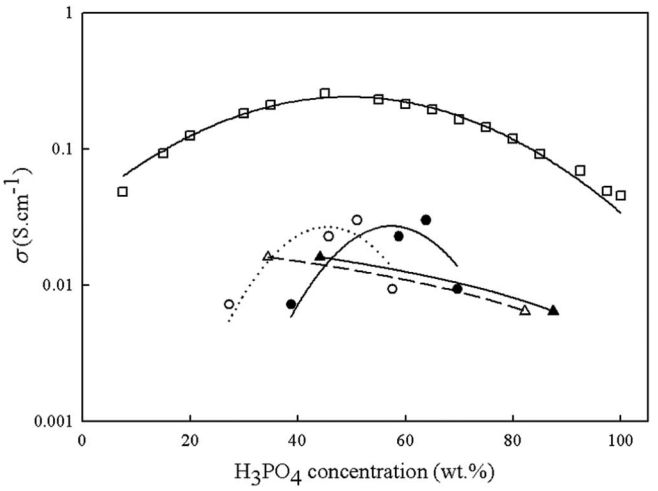

Figure 8. Conductivity of the membranes as a function of the concentration of phosphoric acid inside the membrane, expressed in wt%, compared to phosphoric acid aqueous solution (□),[47] (●) ABPBI-ET ($\lambda_a = 2.5$); (○)ABPBI-ET (λ_a-$[L^1]_T = 1.48$); (▲)ABPBI-MSA ($\lambda_a = 2.8$); (△) ABPBI-MSA (λ_a-$[L^1]_T = 1.78$).

concentration inside the membrane discounting the acid molecules linked to L_1 sites (that is, $[L^1]_T$) is also included in Figure 8.

As it was noticed in Figure 6, the conductivity of ABPBI-ET membranes plotted as a function of the water activity showed a maximum. It can be seen in Figure 8, that a maximum is also present if the conductivity of ABPBI-ET is considered as a function of acid concentration inside the membrane. The maximum in ABPBI-ET occurs at a different acid concentration as compared with that of phosphoric acid aqueous solution. However, both maximum agree rather well when we calculate the acid concentration inside the ABPBI-ET membrane discounting the acid molecules linked to L_1 sites. Hence, it can be concluded that the acid molecules that take part in the proton conduction in ABPBI-ET membranes are those linked to L_2 sites.

For ABPBI-MSA membranes the ionic conductivity vs. membrane acid concentration data are not enough to decide about the existence of a maximum. Indeed, Figure 8 seems to indicate that proton conductivity in ABPBI-MSA decreases slightly with increasing acid concentration, or in other words, the conductivity increases at increasing water content in the membrane. Thus, it is not possible to decide whether only the L_2 sites are responsible for the proton conductivity of this membrane.

The strong dependence of ABPBI-ET conductivity from water activity is indicating that the proton conduction mechanism may be strongly related with the water content and water interaction inside the polymer. ABPBI-ET have shown a high water uptake at $a_w < 0.7$ compared with other ABPBI membranes, as it was discussed above, and GAB analysis had indicated an strong interaction water – polymer in this type of membranes.

In this case, water molecules can be consider as enablers of conduction mechanism, as the acid molecules require water interaction to reorder and reorient themselves in order to enable the proton conduction, as it was pointed out by Vilčiauskas et al.,[48] based in their analysis of the mechanism of electrical conduction of phosphoric acid in aqueous solution by molecular dynamic simulation.

Conclusions

ABPBI-ET membranes were prepared by a new low temperature casting procedure and doped with 10.6 M H_3PO_4. The water uptake and proton conductivity of these membranes were compared with those of membranes prepared from ABPBI by casting at high temperature, PBI, and commercial cross linked ABPBI by Fumatech.

The casting procedure for membrane preparation has a strong influence in the properties analyzed, like doping level, water uptake and conductivity behavior. ABPBI-ET showed higher water uptake than that of PBI all over the range of water activity, and higher than that of ABPBI-MSA at $a_w < 0.7$, with strong interaction of water molecules with ABPBI-ET polymer, indicated by GAB analysis. Supported ultrathin ABPBI-ET membranes, with thickness between 10 nm and 30 nm, exhibited water uptake 3 to 5 times lower than that of massive membranes, probably as a consequence of polymer interaction with the substrate.

The conductivity of the membranes doped in 10.6 M H_3PO_4 increases with increasing temperature. The conductivity of ABPBI-ET membranes showed a different behavior when considered as a function of water activity, with a maximum in $a_w = 0.55$. At this point, the conductivity of this membrane is the highest, with the exception of ABPBI-C membranes doped in 14.9 M H_3PO_4.

The analysis of the proton conductivity behavior based on the basis of the acid dissociation of the PBI or ABPBI complexes with phosphoric acid, using the procedure developed by Scatchard et al., allowed us to conclude that for ABPBI-ET membranes only the acid molecules linked to the -NH- group or linked to another H_3PO_4 molecule by hydrogen bonds play an important role in the proton conduction mechanism. In addition, this mechanism would be strongly influenced by the water content inside the membrane, as far as the water molecules act as enabler of the proton transport.

Finally, it should be emphasized that the proton conductivity of ABPBI-ET membranes are higher than those observed for Nafion membranes over the temperature range analyzed in this work. The proton conductivity of ABPBI-ET membranes is expected to be even higher above 120°C, which is of great relevance for applications in high-temperature PEM fuel cells.

Acknowledgments

The authors acknowledge financial support from ANPCyT (PICT 2097 and PAE 36985), CNEA, and CONICET (PIP 00095). HRC is a member of Consejo Nacional de Investigaciones Científicas y Técnicas (CONICET). GCA and LAD thank financial support of Instituto Nacional de Tecnología Industrial (INTI).

List of Symbols

a_w	water activity
b	membrane width [cm]
c	parameter of GAB equation
E_1	water-polymer interaction energy at the monolayer [kJ.mol^{-1}]
E_2	water-polymer interaction energy at layers top of the monolayer [kJ.mol^{-1}]
E_L	pure water liquefaction energy [kJ.mol^{-1}]
f	parameter of GAB equation
l	distance between measurement electrodes [cm]
K_{a1}	first dissociation constant of H_3PO_4
K_{aL1}	L_1–H_3PO_4 dissociation constant
K_{aL2}	L_2–H_3PO_4 dissociation constant
K_{L1}	L_1–H_3PO_4 complex formation constant
K_{L2}	L_2–H_3PO_4 complex formation constant
L_1	–N = group of the imidazole ring
$[L^1]_T$	limiting doping level of L_1 sites
L_2	–NH– group of the imidazole ring, or other H_3PO_4 molecule
m	water uptake in grams of water per gram of dry polymer
m_a	mass of acid [g]
m_0	mass of water at the monolayer per gram of dry membrane
m_p	mass of dry polymer [g]
m_s	mass of sorbed water [g]
n_a	moles of acid
n_{H2O}	moles of water

M_a	acid molecular weight [g.mol^{-1}]
M_p	molecular weight of the monomer unit containing one imidazole ring [g.mol^{-1}]
M_w	water molecular weight [g.mol^{-1}]
R	electrical resistance of the membrane [S^{-1}]

Greek

δ	membrane thickness [cm]
λ_a	moles of acid per mole of imidazole group
λ_f	free acid content of the membrane
λ_w	moles of water per imidazole group
λ_{wa}	moles of water per mol of acid
σ	specific ionic conductivity of the membrane [S.cm^{-1}]

Subscripts

a	acid
f	free
p	polymer
s	sorbed water
w, H_2O	water
L	liquefaction

References

1. K. A. Mauritz and R. B. Moore, *Chem. Rev.*, **104**, 4535 (2004).
2. J. S. Wainright, J-T. Wang, D. Weng, R. F. Savinell, and M. Litt, *J. Electrochem. Soc.*, **142**, L121 (1995).
3. J. Zhang, Z. Xie, J. Zhang, Y. Tang, C. Song, T. Navessin, Z. Shi, D. Song, H. Wang, D. P. Wilkinson, Z-S. Liu, and S. Holdcroft, *J. Power Sources*, **160**, 872 (2006).
4. R. Savinell, E. Yeager, D. Tryk, U. Landau, J. Wainright, D. Weng, K. Lux, M. Litt, and C. Rogers, *J. Electrochem. Soc.*, **141**, L46 (2004).
5. R. Yadav and P. S. Fedkiw, *J. Electrochem. Soc.*, **159**, B340 (2012).
6. S. Ochi, O. Kamishima, J. Mizusaki, and J. Kawamura, *Solid State Ionics*, **180**, 580 (2009).
7. J. Mader, L. Xiao, T. J. Schmidt, and B. C. Benicewicz, *Adv. Polym. Sci.*, **216**, 63 (2008).
8. J. A. Asensio, S. Borrós, and P. Gómez-Romero, *J. Polym. Sci. Part A: Polym Chem.*, **40**, 3703 (2002).
9. A. Carollo, E. Quartarone, C. Tomasi, P. Mustarelli, F. Belotti, A. Magistris, F. Maestroni, M. Parachini, L. Garlaschelli, and P. P. Righetti, *J. Power Sources*, **160**, 175 (2006).
10. L. Xiao, H. Zhang, E. Scanlon, L. S. Ramanathan, E. W. Choe, D. Rogers, T. Apple, and B. C. Benicewicz, *Chem Mater.*, **17**, 5328 (2005).
11. Z. Liu, Y. -M. Tsou, G. Calundann, and E. De Castro, *J. Power Sources*, **196**, 1055 (2011).
12. H. Pu, Q. Liu, and G. Liu, *J. Membr. Sci.*, **241**, 169 (2004).
13. L. A. Diaz, G. C. Abuin, and H. R. Corti., *J. Membr. Sci.*, **411–412**, 35 (2012).
14. R. Bouchet and E. Siebert, *Solid State Ionics*, **118**, 287 (1999).
15. J. Lobato, P. Cañizares, M. A. Rodrigo, J. J. Linares, and G. Manjavacas, *J. Membr. Sci.*, **280**, 351 (2006).
16. Q. Li, H. A. Hjuller, and N. J. Bjerrum, *J. Appl. Electrochem.*, **31**, 773 (2001).
17. X. Glipa, B. Bonnet, B. Mula, D. J. Jones, and J. Rozière, *J. Mater. Chem.*, **9**, 3045 (1999).
18. J. Lobato, P. Cañizares, M. A. Rodrigo, J. J. Linares, and J. A. Aguilar, *J. Membr. Sci.*, **306**, 47 (2007).
19. J. A. Asensio, S. Borrós, and P. Gómez-Romero, *Electrochem. Commun.*, **5**, 967 (2003).
20. Y. L. Ma, J. S. Wainright, M. Litt, and R. F. Savinell, *J. Electrochem. Soc.*, **151**, A8 (2004).
21. R. He, Q. Li, G. Xiao, and N. J. Bjerrum, *J. Membr. Sci.*, **226**, 169 (2003).
22. R. He, Q. Li, A. Bach, J. O. Jensen, and N. J. Bjerrum, *J. Membr. Sci.*, **277**, 38 (2006).
23. C. Hasiotis, V. Deimede, and C. Kontoyannis, *Electrochim. Acta*, **46**, 2401 (2001).
24. A. Schechter and R. F. Savinell, *Solid State Ionics*, **147**, 181 (2002).
25. D. Mecerreyes, H. Grande, O. Miguel, E. Ochoteco, R. Marcilla, and I. Cantero, *Chem. Mater.*, **16**, 604 (2004).
26. J. Weber, K. D. Kreuer, J. Maier, and A. Thomas, *Adv. Mater.*, **20**, 2595 (2008).
27. Q. Li, C. Pan, J. O. Jensen, P. Noye, and N. J. Bjerrum, *Chem. Mater.*, **19**, 350 (2007).
28. H. Xu, K. Chen, X. Guo, J. Fang, and J. Yin, *J. Membr. Sci.*, **288**, 255 (2007).
29. J. A. Asencio, S. Borrós, and P. Gómez-Romero, *Electrochim. Acta*, **49**, 4461 (2004).
30. J. A. Asensio, S. Borrós, and P. Gómez-Romero, *J. Electrochem. Soc.*, **151**, A304 (2004).
31. J. A. Asensio, S. Borrós, and P. Gómez-Romero, *J. Membr. Sci.*, **241**, 89 (2004).
32. P. Gómez-Romero, J. A. Asensio, and S. Borrós, *Electrochim. Acta*, **50**, 4715 (2005).
33. J. A. Asensio and P. Gómez-Romero, *Fuel Cells*, **5**, 336 (2005).
34. P. Krishnan, J. S. Park, and C. S. Kim, *J. Power Sources*, **159**, 817 (2006).
35. H. J. Kim, S. Y. Cho, S. J. An, and Y. C. Eun,, J. Y. Kim, H. K. Yoon, H. J. Kweon, and K. H. Yew, *Macromol. Rapid Commun.*, **25**, 894 (2004).
36. C. Wannek, W. Lehnert, and J. Mergel, *J. Power Sources*, **192**, 258 (2009).
37. A. L. Gulledge, B. Gu, and B. C. Benicewicz, *J. Polym. Sci. A: Polym. Chem.* **50**, 306 (2012).
38. O. Acar, U. Sen, A. Bozkurt, and A. Ata, *Int. J. Hydrogen Energy*, **34**, 2724 (2009).
39. G. Scatchard, I. H. Scheinberg, and S. H. Armstrong, *J. Am. Chem. Soc.*, **72**, 535 (1950).
40. R. He, Q. Li, J. O. Jensen, and N. J. Bjerrum, *J. Polym. Sci.: Part A: Polym. Chem.*, **45**, 2989 (2007).
41. L. A. Diaz, G. A. Abuin, and H. R. Corti, *J. Power Sources*, **188**, 45 (2009).
42. G. C. Abuin, M. C. Fuertes, and H. R. Corti, *J. Membr. Sci.*, **428**, 507 (2013).
43. E. A. Guggenheim, Clarendon Press, Oxford (1966).
44. V. Murthi, J. Dura, S. Satija, C. Majkrzak, T. Fuller, K. Shinohara, V. Ramani, P. Shirvanian, H. Uchida, S. Cleghorn, M. Inaba, S. Mitsushima, P. Strasser, H. Nakagawa, H. Gasteiger, T. Zawodzinski, and C. Lamy, *ECS Transactions* **16**, 1471 (2008).
45. J. A. Dura, V. S. Murthi, M. Hartman, S. Satija, and C. F. Majkrzak, *Macromolecules*, **42**, 4769 (2009).
46. R. He, Q. Che, and B. Sun, *Fiber. Polym.*, **9**, 679 (2008).
47. C. M. Mason and J. B. Culvern *J. Amer .Chem. Soc.*, **71**, 2387 (1949).
48. L. Vilčiauskas, M. E. Tuckerman, G. Bester, S. J. Paddison, and K. D. Kreuer, *Nat. Chem.*, **4**, 461 (2012).